

Multiparticle SUSY simulations at LHC & ILC: Off-Shell effects, interferences and radiative corrections

Jürgen Reuter ^a

University of Freiburg, Institute of Physics, Germany

Abstract. The interesting but difficult phenomenology of supersymmetric models at the LHC and ILC demands a corresponding complexity and maturity from simulation tools. This includes multi-particle final states, reducible and irreducible backgrounds, spin correlations, real emission of photons and gluons, virtual corrections etc. Most of these topics are included in the multi-particle Monte Carlo (MC) Event generators Madgraph, WHIZARD and Sherpa. A comparison of these codes is shown, with a special focus on the new release of WHIZARD. I show examples for the necessity of considering full matrix elements with all off-shell effects and interferences for multi-particle final states in supersymmetric models and give a status report on ongoing projects for simulations of SUSY processes at the LHC with these codes, including all of the abovementioned corrections.

PACS. 11.30.Pb Supersymmetry – 12.38.Bx Perturbative Calculations – 12.60.Jv Supersymmetric models

1 The need for multi-particle event generators

Supersymmetry (SUSY) is the prime example for beyond the Standard Model (SM) physics as a solution to the hierarchy problem. Compared to the SM, it doubles the particle spectrum, and the SUSY-breaking terms induce a vast number of new parameters. The analysis goal of the future experiments at the LHC and an ILC include mass measurements to determine the SUSY spectrum, the access of the new particles' spin encoded in angular correlations, and finally, by means of coupling measurements the proof that the new particles really fill super-multiplets. Together with the complicated experimental set-up to dig out the informations mentioned above, there is an utter need for precise theoretical predictions of SUSY processes: first of all, to access them from the SM background, secondly since SUSY processes are themselves backgrounds for (more complicated) SUSY processes. Ultimately, the goal is to extract the SUSY Lagrangian parameters as precisely as possible to make predictions about the GUT structure and the SUSY breaking mechanism [1].

In general, corrections to SUSY (or in general BSM) processes can be grouped into six categories: 1) loop corrections to SUSY production and decay processes, 2) real gluon/photon radiation, 3) non-factorizable, maximally resonant photon exchange between production and decay, 4) off-shell kinematics for the signal process, 5) irreducible background from all other SUSY processes, and 6) reducible, but experimentally indis-

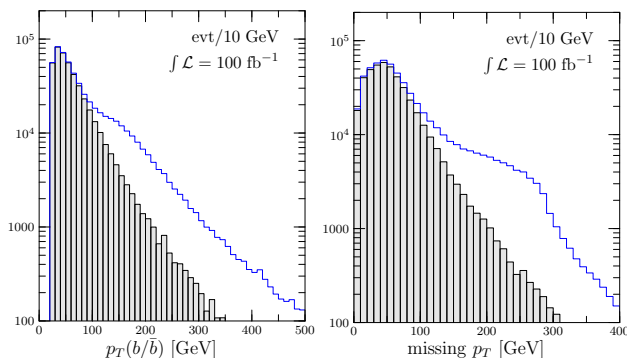


Fig. 1. $p_T(b)$ and missing p_T distribution for the process $pp \rightarrow b\bar{b}\tilde{\chi}_1^0\tilde{\chi}_1^0$ resulting from sbottom pair production at the LHC. The SM background is in grey, the signal in blue.

tinguishable background from SM processes. Topics 1) and 3) are dealt with in [2]. Here, we will focus on the last three points.

SUSY processes reach a very high level of complexity already at tree level: e.g. the process $e^+e^- \rightarrow b\bar{b}e^+e^-\tilde{\chi}_1^0\tilde{\chi}_1^0$ – which is just $\tilde{\chi}_2^0\tilde{\chi}_2^0$ pair production – has $\sim 66,500$ Feynman diagrams. Several different production channels like $\tilde{\chi}_i^0\tilde{\chi}_j^0$, $\tilde{b}_i\tilde{b}_j^*$ and $\tilde{e}_i\tilde{e}_j^*$ interfere with each other and need to be disentangled experimentally as well as in the simulation. One has to add SM backgrounds like $e^+e^- \rightarrow b\bar{b}e^+e^-\nu\bar{\nu}$. And processes can be much more complicated at the LHC, but also at the ILC. To make simulation of such complicated multi-particle processes feasible, among the following three levels of complexity usually one of the two first are

^a Email: juergen.reuter@desy.de

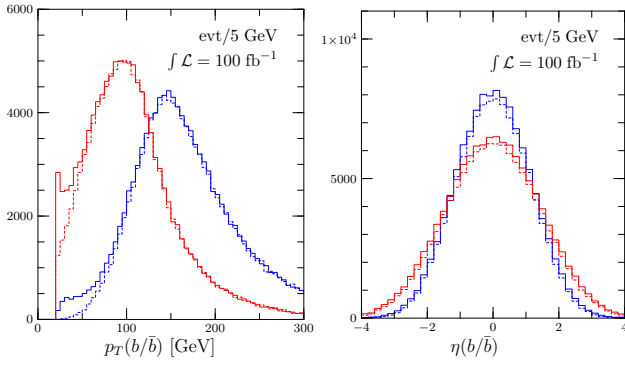


Fig. 2. Process: $pp \rightarrow b\bar{b}\tilde{\chi}_1^0\tilde{\chi}_1^0$, distributions of the harder and softer b jet in red and blue, respectively: on the left p_T , on the right in η . Full lines are full matrix elements, dashed ones Breit-Wigner approximation.

used: first, there is the narrow-width approximation (NWA), where intermediate states are produced on-shell and multiplied by the corresponding branching ratio. Secondly, there is the Breit-Wigner approximation (BWA), where the on-shell state's width is accounted for by folding in a Breit-Wigner propagator. Finally, there are the full matrix elements including all intermediate off-shell states contributing to the same exclusive final state. Programs like PYTHIA, HERWIG, SUSYGEN and ISAJET use the first two approaches. Here, we will show that this is not sufficient and that for BSM models full matrix elements have to be used.

2 SUSY simulations at the LHC

For simulations of multi-particle SUSY processes at the LHC, the three packages WHIZARD [3,4], Sherpa [5] and Madgraph [6] have been developed. All of these programs follow the SUSY Les Houches accord (SLHA) [7]. Since the MSSM is a fairly complicated model with several thousand different vertices, it is mandatory to validate the correctness of its implementation in the codes. This has been done in [8] by means of unitarity and gauge invariance checks as well as a direct comparison of the three programs. To test all phenomenologically relevant couplings, more than 500 different processes had to be checked; they are listed here [8, 9], which might serve as a standard reference. Furthermore, supersymmetric Ward- and Slavnov-Taylor identities have been checked [10].

To study the influence of interferences and off-shell effects as well as of radiative corrections, we chose a mSUGRA-inspired parameter point with non-universal scalar masses (note that the following discussion does by no means depend on that special point). The sbottom masses are 295 and 400 GeV, respectively, the lightest Higgs is directly above the LEP exclusion limit. It has a large (47 %) branching ratio of invisible decays to the neutralino LSP. The first generation squarks and sleptons are at 430 and 205 GeV, respectively. The point is compatible with all low-energy constraints like

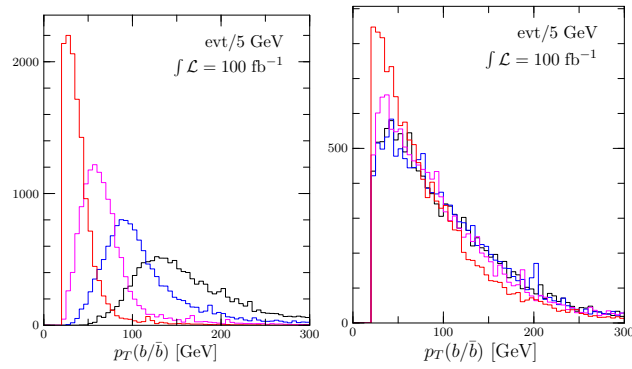


Fig. 3. p_T distributions of the four b jets in the process $pp \rightarrow b\bar{b}b\bar{b}\tilde{\chi}_1^0\tilde{\chi}_1^0$, on the left: ordered according to their p_T , on the right: ordered according to their centrality.

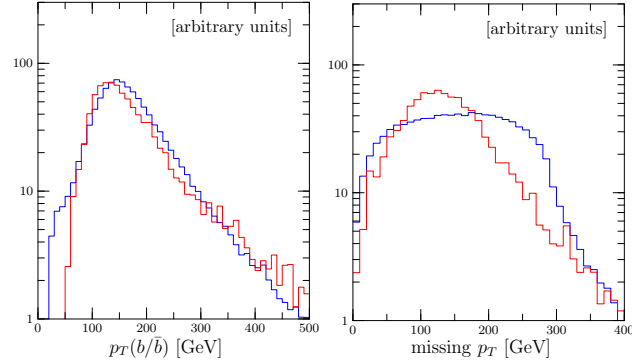


Fig. 4. $p_{T,b}$ and \cancel{p}_T distributions for the processes with two b jets in blue and with four b jets in red.

$b \rightarrow s\gamma$, $B_s \rightarrow \mu^+\mu^-$, $\Delta\rho$, $g_\mu - 2$, and cold dark matter. The focus here lies on sbottom production with a $\text{BR}(\tilde{b}_1 \rightarrow b\tilde{\chi}_1^0) = 43.2\%$.

Fig. 1 shows the parton-level distributions for $pp \rightarrow b\bar{b}\tilde{\chi}_1^0\tilde{\chi}_1^0$, where we used standard cuts of $p_{T,b} > 20$ GeV, $\eta_b < 4$, and $\Delta R_{bb} > 0.4$. The main SM background comes from $pp \rightarrow b\bar{b}\nu\bar{\nu}$ and is shown in gray. The signal is in blue, the $p_{T,b}$ distribution on the left, the \cancel{p}_T distribution on the right. Here, the bump coming from the sbottom production is clearly visible. Generally, the signal jets are harder than the jets from the SM background. In Fig. 2, the $p_{T,b}$ and η_b distributions are plotted for the harder (red) and the softer (blue) of the two jets. From the right plot we see that the harder jet is much more central as expected from phase space restrictions. The full lines here denote usage of full matrix elements, while the dashed lines are the BWA. There is a clear discrepancy between the curves, stemming mainly from $b\bar{b}Z^*$ diagrams; these discrepancies are only in the low- p_T region which is anyhow cut out. The reason why off-shell decays are irrelevant here is the large mass splitting from 295 to 45 GeV between the sbottom and the LSP. For general SUSY decay cascades this is not the case as will be explained in section 4.

As a next step, we studied the influence of real corrections on the detection of the signal, i.e. bottom-jet radiation from the initial state ($g \rightarrow b\bar{b}$ splitting) as

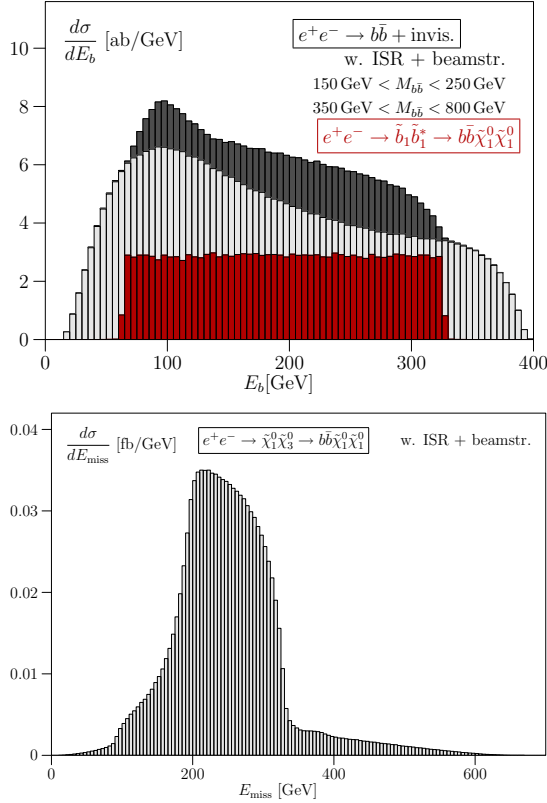


Fig. 5. Top: energy of the b jet in the process $e^+e^- \rightarrow b\bar{b} + E$ at the ILC. In red the NWA, in light gray the SM background, and in dark gray the signal with full matrix elements on top of it. ISR and beamstrahlung are included. Bottom: same, but E distribution.

combinatorial background. Using the above cuts for the b jets, the perturbation series is well-behaved, the cross section ceases from 1177 fb to 130.7 fb when including the two bottom jets. The process with four b jets, $pp \rightarrow b\bar{b}b\bar{b}\tilde{\chi}_1^0\tilde{\chi}_1^0$, is at the border of feasibility for SUSY LHC simulations with 32,000 diagrams, 22 color flows and several thousand phase space channels. The simulation has been performed with WHIZARD, which is well-suited for physics beyond the SM [11]. Fig. 3 shows the p_T distributions of the four b jets, ordered according to their p_T on the left and to their pseudorapidity on the right. The right figure shows that only the most forward jet is considerably softer, and that a forward discrimination between ISR and signal (decay) jets can be quite intricate. Fig. 4, on the other hand, shows that the jet structure (left hand side) itself does not change considerably from the case with two (blue) and four b jets (red). Since more hard jets have to be produced, the PDFs decrease the maximum a little bit. The missing p_T is shifted to lower values because light particles balance out the event.

3 SUSY simulations at the ILC

At the ILC, we consider the same final state, $e^+e^- \rightarrow b\bar{b}\tilde{\chi}_1^0\tilde{\chi}_1^0$. Here, the production is electroweak, whence

a lot more of intermediate states contribute: $Zh, ZH, HA, \tilde{\chi}_1^0\tilde{\chi}_2^0, \tilde{\chi}_1^0\tilde{\chi}_3^0, \tilde{\chi}_1^0\tilde{\chi}_4^0, \tilde{b}_1\tilde{b}_1^*, \tilde{b}_1\tilde{b}_2^*$. Especially, the background from heavy Higgses and the heavier neutralinos is quite severe. The irreducible SM background is mainly from WW fusion: $e^+e^- \rightarrow b\bar{b}\nu\bar{\nu}$. To extract the sbottom from the SUSY backgrounds, one has to cut out the regions in the $M_{b\bar{b}}$ spectrum from 150 to 250 GeV as well as from 350 to 800 GeV. Applying these cuts, the result for the cross section of the signal is 0.487 fb (0.375 fb with ISR and beamstrahlung); the NWA gives 2.314 fb, which is one order of magnitude away from the full result. The reason is that interferences with heavy neutralino three-body decays affect the decay kinematics of the sbottoms. Hence, for ILC it is absolutely mandatory to use full matrix elements and multi-particle event generators for SUSY simulations.

4 Origin of off-shell effects

In this section, we briefly explain the reason for the appearance of large off-shell and interference effects for SUSY processes at the LHC (for a clear derivation of these effects, see [12]). Although, here we focus on SUSY, all new physics scenarios which have a conserved matter parity (responsible for dark matter) and a complicated spectrum without too large hierarchies in common, share the same features. Their phenomenology grossly consists of decay chains with quasi-degeneracies among mother and daughter particles. Including the full momentum dependence of the decay matrix elements affects the momentum dependence of the propagators: performing phase space integrals does not result in simple Breit-Wigner terms that factor out. Although naively, the importance of off-shell effects is expected to scale with the width to mass ratio Γ/M for the resonances, these factors can be largely enhanced by powers of the (small) inverse velocity of the daughters, $1/\beta^n$, coming from the near-degeneracies of mothers and daughters. Furthermore, interferences with diagrams where only one of the two decay chains is resonant can be quite large.

Altogether, these effects lead to drastic deviations from the NWA: effective branching ratios (which are measured via their exclusive final states) are shifted by 20 – 40 %. Charge and chirality asymmetries could appear in the decays of gluinos: e.g. $\tilde{g}\tilde{g} \rightarrow b\bar{b}^*b\bar{b}^*$ vs. $\tilde{b}_1\tilde{b}_1^* \rightarrow b\bar{b}^*b\bar{b}^*$ could have different effective branching ratios since they have different subsequent decay chains which have different interferences with non-resonant diagrams. A chirality asymmetry is a non-equality between the two decays $\tilde{g}\tilde{g} \rightarrow \tilde{q}_L\tilde{q}_Ljj$ vs. $\tilde{q}_R\tilde{q}_Rjj$ for the same reasons as above.

In Fig. 6 (taken from [12]) the effect of using full matrix elements are shown for the process $u\bar{d} \rightarrow \tilde{\chi}_1^+\tilde{g}$ with subsequent decays of the gluino. The left plot shows the deviations of the effective branching ratios for the gluino measured with the help of exclusive final states as a function of the ratio of the squark over the gluino mass. As this ratio approaches one, off-shell

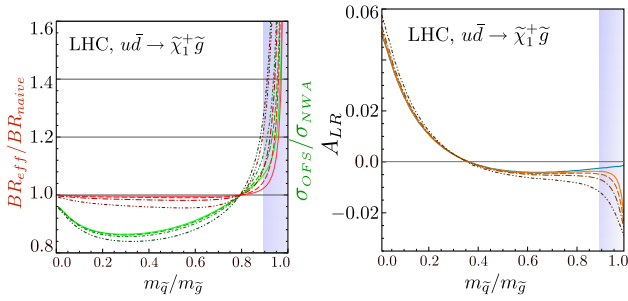


Fig. 6. Off-shell and interference effects for SUSY decay chains at the LHC. Left: shifts to the gluino BR as a function of $m_{\tilde{q}}/m_{\tilde{g}}$. Right: Decay asymmetry $(\tilde{g} \rightarrow \tilde{q}_L q)/(\tilde{g} \rightarrow \tilde{q}_R q)$; from [12]. The shaded blue area covers all SPS points.

and interference effects give corrections of the order of 20–40 % compared to the NWA. This near-degenerate squark-gluino parameter region is quite generic, since all SPS-standard candle points [13] lie in the blue band. So for all of these points, there are large deviations from the NWA. The right plot shows a chirality asymmetry, i.e. an asymmetry between the decays $\tilde{g} \rightarrow \tilde{q}_L q$ and $\tilde{g} \rightarrow \tilde{q}_R q$.

In [14], all of the off-shell and interference effects discussed briefly above, are studied systematically for all kinds of different SUSY decay chains and observables. Also, the size of these effects as a function of the region of parameter space is investigated.

5 Conclusions

In conclusion, we validated the three multi-particle event generators for MSSM processes, Madgraph, Sherpa, and WHIZARD, to produce correct results. We studied the influence of using full matrix elements for exclusive four- and six-particle final states in SUSY production processes at the LHC and ILC compared to the narrow-width or Breit-Wigner approximation. If there are several different diagram classes that can become singly- or doubly-resonant, interferences of these classes result in deviations from the NWA up to an order of magnitude. Furthermore, off-shell effects are important for nearly-degenerate mother-daughter constellations, as is typical in SUSY decay chains (but also in all BSM scenarios with a conserved parity and similar spectra). Especially, when cuts are mandatory to disentangle signals and backgrounds, interference and off-shell effects have to be studied by multi-particle event generators.

6 Acknowledgments

JR was partially supported by the Helmholtz-Gemeinschaft under Grant No. VH-NG-005 and the Bundesministerium für Bildung und Forschung, Germany, under Grant No. 05HA6VFB. Special thanks to David Rainwater for his close collaboration and providing the plots in Fig. 6.

References

1. <http://spa.desy.de/spa>; J. A. Aguilar-Saavedra *et al.*, Eur. Phys. J. C **46**, 43 (2006).
2. T. Robens, these proceedings; W. Kilian, J. Reuter and T. Robens, Eur. Phys. J. C **48**, 389 (2006); AIP Conf. Proc. **903**, 177 (2007)
3. T. Ohl, *O'Mega: An Optimizing Matrix Element Generator*, hep-ph/0011243; M. Moretti, T. Ohl, J. Reuter, hep-ph/0102195; J. Reuter, arXiv:hep-th/0212154.
4. <http://whizard.event-generator.org>; W. Kilian. LC-TOOL-2001-039, Jan 2001; W. Kilian, T. Ohl, J. Reuter, to appear in Comput. Phys. Commun., arXiv:0708.4233 [hep-ph].
5. <http://www.sherpa-mc.de>; F. Krauss, R. Kuhn and G. Soff, JHEP **0202**, 044 (2002); T. Gleisberg, S. Höche, F. Krauss, A. Schälicke, S. Schumann and J. C. Winter, JHEP **0402**, 056 (2004).
6. <http://madgraph.hep.uiuc.edu>; H. Murayama, I. Watanabe and K. Hagiwara, KEK-91-11; T. Stelzer, F. Long, Comput. Phys. Commun. **81** (1994) 357; F. Maltoni and T. Stelzer, JHEP **0302** (2003) 027.
7. P. Skands *et al.*, JHEP **0407**, 036 (2004).
8. K. Hagiwara *et al.*, Phys. Rev. D **73**, 055005 (2006); J. Reuter *et al.*, arXiv:hep-ph/0512012; J. Reuter, arXiv:0709.0068 [hep-ph].
9. http://whizard.event-generator.org/susy_comparison.html
10. T. Ohl and J. Reuter, Eur. Phys. J. C **30**, 525 (2003).
11. W. Kilian and J. Reuter, Phys. Rev. D **70** (2004) 015004; W. Kilian, D. Rainwater and J. Reuter, Phys. Rev. D **71**, 015008 (2005); hep-ph/0507081; Phys. Rev. D **74**, 095003 (2006); M. Beyer *et al.*, Eur. Phys. J. C **48**, 353 (2006); W. Kilian and J. Reuter, hep-ph/0507099; J. Reuter, arXiv:0708.4241 [hep-ph]. T. Ohl and J. Reuter, Phys. Rev. D **70**, 076007 (2004); arXiv:hep-ph/0407337; W. Kilian and J. Reuter, Phys. Lett. B **642**, 81 (2006); F. Deppisch, W. Kilian, J. Reuter, in preparation.
12. D. Berdine, N. Kauer and D. Rainwater, to appear in Phys. Rev. Lett., arXiv:hep-ph/0703058.
13. B. C. Allanach *et al.*, in *Proc. of the APS/DPF/DPB Summer Study on the Future of Particle Physics (Snowmass 2001)* ed. N. Graf, Eur. Phys. J. C **25**, 113 (2002); N. Ghodbane and H. U. Martyn, in *Proc. of the APS/DPF/DPB Summer Study on the Future of Particle Physics (Snowmass 2001)* ed. N. Graf, arXiv:hep-ph/0201233.
14. A. Alboteanu, J. Alwall, W. Kilian, T. Plehn, D. Rainwater, J. Reuter, S. Schumann, in preparation.